

Real-Time, High-Accuracy 3D Tracking of Small Animals for Motion-Corrected SPECT Imaging

S. S. Gleason, *Member, IEEE*, J. S. Goddard, *Member, IEEE*, M. J. Paulus, *Member, IEEE*, J. S. Baba, S. Majewski, M. Smith, *Member, IEEE*, T. Tran, A. Weisenberger, B. Welch, R. Wojcik

Abstract--An optical landmark-based pose measurement and tracking system has been developed to provide 3D animal position data for a single photon emission computed tomography (SPECT) imaging system for non-anesthetized, unrestrained laboratory animals. The animal position and orientation data provides the opportunity for motion correction of the SPECT data. The tracking system employs infrared (IR) markers placed on the animal's head along with strobed IR LEDs to illuminate the reflectors. A stereo CMOS camera system acquires images of the markers through a transparent enclosure. Software routines segment the markers, reject unwanted reflections, determine marker correspondence, and calculate the 3D pose of the animal's head. Recent improvements have been made in this tracking system including enhanced pose measurement speed and accuracy, improved animal burrow design, and more effective camera positioning for enhanced animal viewing. Furthermore, new routines have been developed to calibrate the SPECT detector head positions relative to one another and to align the coordinate systems of the optical tracking cameras with the SPECT detectors. This alignment enables motion-corrected SPECT image reconstruction. Phantom experiments validate the accuracy of the tracking system to better than 0.1mm accuracy, and live mouse tracking results demonstrate that reliable, accurate tracking measurements can be consistently achieved during the entire 360-degree SPECT image acquisition.

I. INTRODUCTION

SMALL animal tomographic imaging using nuclear medicine-based technologies [e.g. single-photon emission tomography (SPECT) or positron emission tomography (PET)] have enabled researchers to acquire *in vivo* images of the biodistribution of radio labeled molecules in animal models. A common problem encountered by researchers using this technology is that the use of anesthetic or physical restraints has the potential to alter the neurological and physiological processes that are under study. For this reason, the Department of Energy's Oak Ridge National Laboratory (ORNL) and Thomas Jefferson National Accelerator Facility (Jefferson Lab), in collaboration with Royal Prince Alfred Hospital in Sydney, Australia have been developing a high-resolution SPECT system to image unrestrained, un-anesthetized small laboratory animals [1].

As part of this effort, ORNL has been developing an optical-based animal position tracking apparatus which was introduced in [2]. In summary, the tracking system consists of

a pair of CMOS cameras¹ and an IR strobe system that are used to illuminate and capture images of a set of IR retro reflective markers affixed to the animal's head. Software was written to segment the markers, determine their correspondence, and then calculate the overall position and orientation (pose) of the animal's head over time to provide time-stamped corrections for the SPECT data. A gantry was designed that can accommodate a rotating set of two SPECT detectors as well as a fixed stereo-based optical camera system. A top-down view of the system concept is shown below in Fig. 1.

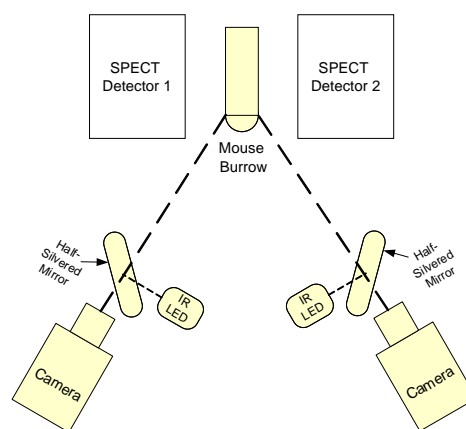


Fig. 1. Optical tracking/SPECT system concept. A stereo pair of CMOS cameras is viewing a burrow in which the animal resides during the SPECT acquisition. Strobed IR sources provide motion-freezing illumination of the IR marker on the animal's head. Two SPECT detectors rotate about the animal during the scan.

This paper describes recent improvements made to this tracking system including enhanced pose measurement speed and accuracy, improved animal burrow design, and more effective camera positioning for enhanced animal viewing. Also, new routines were developed to calibrate the SPECT detector head positions relative to one another and to align the coordinate systems of the optical tracking cameras with the SPECT detectors to enable motion-corrected SPECT reconstruction. Phantom experiments validate the accuracy of the tracking system to better than 0.1mm accuracy, and live mouse tracking results demonstrate that reliable, accurate

tracking measurements can be consistently achieved during the entire 360-degree SPECT image acquisition

II. DESCRIPTION OF SYSTEM

The photograph in Fig. 2 shows the mounting locations of the SPECT detectors and animal burrow with the tracking cameras and optics. The SPECT detectors were designed and fabricated by the Detector Group at Jefferson Lab and are described in detail in [3]. Two high-speed CMOS cameras are mounted at a 15-degree angle above the SPECT gantry axis of rotation. The cameras' positions are angled to look slightly down on top of the head of the animal in order to improve visibility of the upper head area where at least three IR retro reflective markers are fastened to the animal. The markers require that the illumination be directed coaxially along the camera's optical axis. Anti-reflective (AR) coating has been applied to the animal burrow, and polarizing filters can be used to eliminate reflections off the surface of the glass burrow. At this point AR coating has only been applied to the outside of the burrow, so there are still some dim reflections off of the inside surface of the burrow that must be handled appropriately in the software (described in section III). The markers are spherical with one small flat spot suitable for attaching to the head. The LED arrays are strobed for sub-millisecond durations in sync with the image frame acquisition from the cameras. This provides both simultaneous image acquisitions from the two cameras as well as blur-free images.

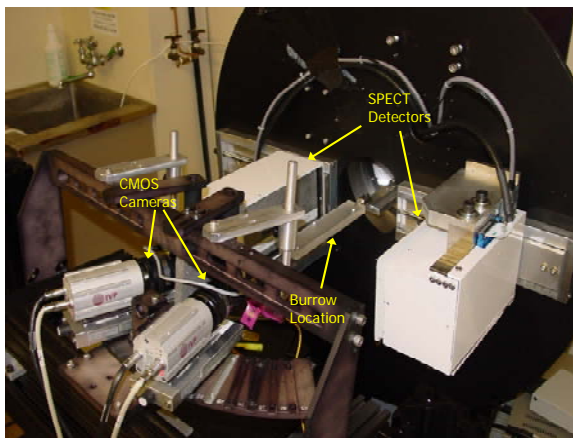


Fig. 2. SPECT gantry with optical tracking system layout.

The overall system architecture including the SPECT gantry, the tracking system, the SPECT motion control system, and the detector data acquisition system is shown in Fig. 3. Three separate computers are used in this system: (1) a motion control PC controls the rotating SPECT gantry, (2) an optical tracking PC processes the data coming from the optical tracking cameras, processes the images, and measures the pose of the animal, and (3) the SPECT data acquisition PC controls the SPECT detector readout and storage of the list mode data.

Note that each PC writes out data files that are time-stamped using a central system clock that distributes the same time to all three PCs. These time-stamped data files are then post processed to perform motion corrected SPECT reconstruction.

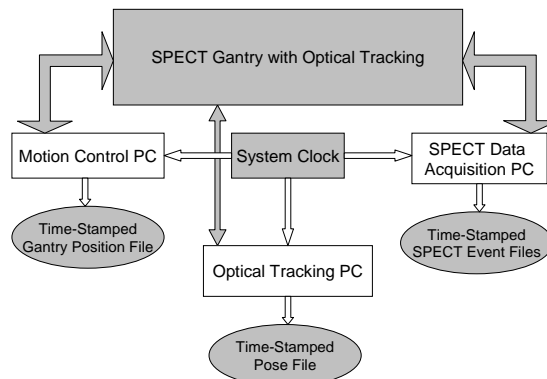


Fig. 3. Overall system architecture of SPECT system with motion correction.

III. MEASUREMENT APPROACH

This section details the tracking approach that has been implemented. The first step is to accurately calibrate the system, which involves three separate calibrations that are described here in detail. Second, the methodology for real time pose measurement is presented. Lastly, significant improvements in the tracking system's speed and accuracy are described.

A. Calibration

This section describes three calibrations that must be performed to ensure accurate tracking, SPECT imaging, and gamma event correction based on pose data.

First, intrinsic and extrinsic optical tracking camera calibration is performed offline and is automated through the use of a planar target with a checkerboard pattern. Intrinsic camera calibration calculates the internal camera parameters that include effective lens focal length, optical center, and lens distortion. Extrinsic calibration is needed to determine the position of the stereo cameras with respect to one another. A complete description of the intrinsic and extrinsic calibration process is given in [2] and [4].

Second, for a high resolution SPECT imaging system, it is important that acquisition geometry be accurately determined. A small deviation from an assumed geometry can degrade reconstructed image resolution. For a SPECT detector equipped with a single pinhole collimator, a model of projection geometry can be characterized by 7 parameters [5]. These parameters include collimator focal length, distance from pinhole to axis of rotation, detector orientations with respect to a source coordinate system defined by the axis of rotation and the normal ray through the pinhole, and electronic shifts in the detector. The projection model for a SPECT detector equipped with a parallel-hole collimator needs only five of the above mentioned seven parameters (excluding focal

length and distance from pinhole to axis of rotation). Parameter values can be accurately determined by fitting the two projection models simultaneously to projection data measured over 360 degrees of rotation. Projections were obtained using a calibration phantom containing three point sources in a triangular configuration [6]. The positions of the point sources are also fitted. Their initial positions are updated with a constraint that the distances between point source remain the same. This positional adjustment amounts to a correction using 3 orthogonal translations and 3 rotations. A total of eighteen parameters are fitted. The least-squares parameter estimates were obtained by an iterative downhill simplex routine.

Thirdly, the coordinate systems of the optical tracking system and the SPECT detector system must be aligned so that pose measurements made in the optical frame can be used to correct the position of the gamma events recorded by the SPECT detectors. Calibration phantoms have been designed for simultaneous calibration of the SPECT gamma cameras and the tracking cameras. Co-57 point sources and retro reflective markers are mounted on a Lucite block at precise locations so that the offsets between the markers and the sources are known accurately (see Fig. 4).

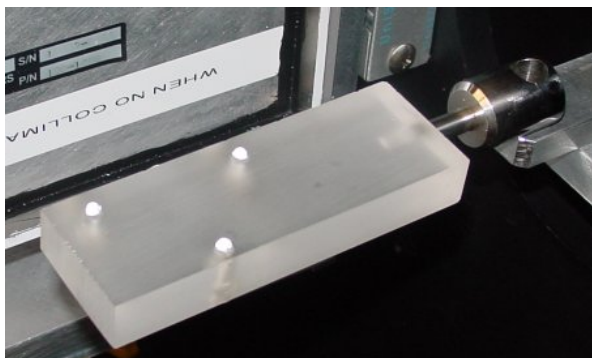


Fig. 4. Calibration phantom for aligning SPECT detectors and the coordinate systems of the SPECT and optical tracking systems. The silver hemispheres are the IR reflective markers. Embedded in the lucite block directly beneath each of the reflectors are the Co-57 point sources.

During a calibration scan, the calibration phantom is fixed within the field of view of the gamma cameras and a 360 degree SPECT scan is taken. At the same time the tracking cameras measure the coordinate frame transformation between the markers coordinates as given by,

$$m_{TC} = T_{P-TC} m_P, \quad (1)$$

where, T_{P-TC} is the homogeneous transformation matrix between the phantom and tracking camera coordinate reference frames and m_{TC} , m_P are the 3-D coordinate vectors of the markers in the tracking camera and phantom reference frames, respectively. From the SPECT data, the 3-D coordinates of the point sources are determined in the gamma

camera reference frame x_{GC} . Applying the translation offset between the markers and the point sources, the tracking camera system calculates the 3-D coordinates of the markers, x_{TC} , with respect to the tracking camera reference frame using T_{P-TC} . From these two sets of 3-D coordinates the coordinate transformation between the tracking camera reference frame and the gamma camera reference frame, T_{GC-TC} , is determined by a least square fit of the two sets of points using a method given by Horn [7]. The resulting equation is given by

$$x_{TC} = T_{GC-TC} x_{GC}, \quad (2)$$

This calculated transformation is applied during SPECT scans with animal tracking to register the measured coordinates to a common reference frame.

B. Pose Measurement

The pose measurement procedure is detailed in [2], but summarized here for completeness. From each acquired image of the retro-reflective markers, the marker regions are segmented using seeded region growing and the centroid of each is calculated. A minimum of three points is required although more are desirable for redundancy and accuracy. The fundamental matrix and the correspondence condition are used to assign matches between the points in each image by finding the minima in each row and column of an n point match matrix where n is the number of points in each image. For each valid point found, the 3D coordinates relative to the second camera are transformed to the frame of the reference camera so that all coordinates are referenced to the same frame. The image plane coordinates and camera origin define a 3D line for each camera and marker point. These lines when extended to the 3D point location approach each other but are likely to be skew and do not intersect due to noise and measurement error. The midpoint of the line connecting the closest points of approach for these two 3D lines defines the location of the marker point. The result from this measurement is a set of 3D coordinates relative to the reference camera. While one or more points can define a translation between the reference camera and the head reference frame, three or more are needed to define an orientation plane so that the three rotation parameters can be calculated. A 3D model is defined for this head-centered frame and a best fit of 3D points to the model is used to determine the correct point assignment. Horn's method is used to calculate the transformation and resulting error [7]. The complete pose of the mouse frame with respect to the camera is then calculated.

C. Tracking Speed and Accuracy Improvements

The speed of the tracking system has been improved through software optimization. This optimization has been achieved by writing pieces of the tracking algorithm software in a more efficient manner. Also, compiler optimization

settings have been changed to improve execution speed of the segmentation algorithm. These efforts have resulted in an increase in tracking speed from 9 to 15 measurements per second.

A problem that has limited the tracking accuracy is the presence of IR LED reflections off of the inner surface of the animal burrow that can confound the region growing segmentation routine that automatically locates the IR markers in each camera view. The nuisance reflections can be filtered out and ignored unless they happen to merge with the reflections of interest coming from the IR markers. The LED reflections are now filtered based on an image processing measurement of the reflection's size (they are typically smaller than the IR markers) and their aspect ratio (they are more elongated than the IR markers). If these LED reflections merge with the IR marker signal, then these reflections cannot be filtered, and the result is a slight shift in the calculated centroid of the merged signals. Using an optimal triangulation method based on [8], the 3D position of the marker centroids are corrected to minimize the geometric error subject to the epipolar constraint.

The true projection of a 3-D point onto each stereo camera image plane is somewhere on a pair of corresponding epipolar lines for the two cameras and subject to the epipolar constraint, $x_1^T F x_2 = 0$, where F is the fundamental matrix. However, in practice the measured points, x_{m1} , x_{m2} will have error at distances d_1 , d_2 respectively from the epipolar lines in the image plane as shown in Fig. 5. The optimum 3-D point assuming Gaussian image plane noise has projected points x_1 , x_2 . These points are found by minimizing the sum of the squared distances, $d_1^2 + d_2^2$, to the epipolar lines. These distances can be expressed in terms of the epipolar lines and the fundamental matrix. Hartley parameterizes the epipolar lines in terms of a single variable t so that the cost function can be reduced to finding the minimum of a function with one variable. For the epipolar line parameterization, $l_i(t)$, the cost function is

$$\min_t \sum = d_1(x_{m1}, l_1(t))^2 + d_2(x_{m2}, l_2(t))^2. \quad (3)$$

An inverse projection is then used to calculate the 3-D coordinates as the midpoint of the minimum distance line between the two possibly skew lines from the image plane points and the optical axis center.

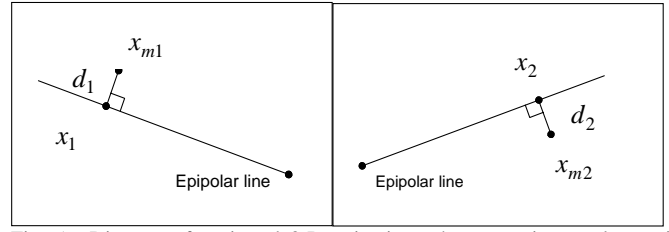


Fig. 5. Diagram of projected 3-D point in each camera image along with measured point showing projection error.

For each matched point, the 3D coordinates are then calculated and transformed to a base reference coordinate frame of the reference camera. These points are matched to a predefined topographic model so that both position and orientation may be calculated.

IV. EXPERIMENTAL RESULTS

A six degree-of-freedom test fixture has been incorporated into the gantry design so that measurement of accuracy can be made in all translations and orientations. Results to date show that accuracies to 0.1 mm for translations and 0.5 degree for rotations have been obtained. A phantom containing three capillary tubes filled with I-125 was mounted onto the six-degree-of-freedom motion stage. Fig. 6 shows the measured versus the actual translation along the axis of rotation of the SPECT imaging system. The system performed similarly in terms of tracking motion in the other degrees of freedom.

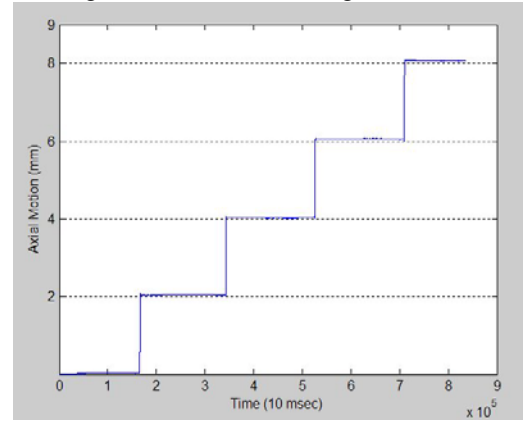


Fig. 6. Plot showing actual (dotted lines at 2, 4, 6, and 8 mm) and measured position (blue points) of a three-rod I-125 phantom.

Extensive live animal tests on mice have been performed, and the system is able to successfully track head motion 99% of the time during a 20-30 minute scan. The animal is anesthetized for a short time to allow affixation of the IR markers to the head of the animal. The animal is then allowed to wake up prior to being placed in the burrow. A photograph of an awake animal in the burrow during a live tracking experiment is shown in Fig. 7. The images in Fig. 8 show the result of automatic segmentation and correspondence calculation of the three markers from each of the two CMOS cameras for this same experiment.



Fig. 7. Mouse with IR reflectors within the AR-coated SPECT imaging burrow.

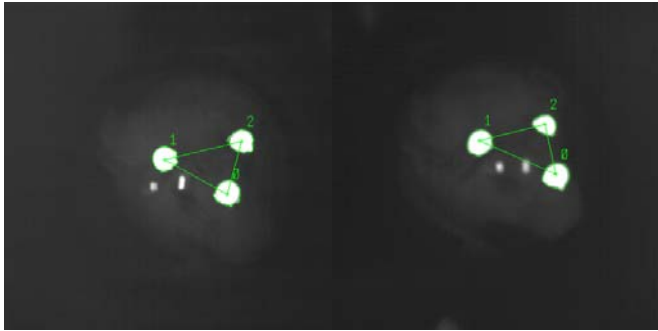


Fig. 8. Raw images acquired simultaneously (left: camera #1, right: camera 2) with the stereo camera pair. The green boundaries around each reflector show the segmentation result, and the numbers are used to label the corresponding marker in each pair of stereo images. The mouse's head is visible in the background.

V. SUMMARY AND FUTURE PLANS

Significant improvements have been made to a stereo camera-based animal head tracking system to allow more accurate reconstruction of SPECT images of non-anesthetized, unrestrained animals. Optimization of the code resulted in an increase in speed from 9 to 15 measurements per second. The accuracy of the system has been improved to better than 0.1mm spatial position accuracy through the use of (1) more intelligent marker centroid calculations to eliminate the error induced by IR LED reflections and (2) more appropriate positioning of the stereo cameras and IR markers on the head of the animal. Finally, the calibration of the system has been enhanced to include accurate determination of the SPECT detector head geometry and calculation of the alignment between the tracking camera coordinate system and the SPECT detectors. Live animal studies are being performed in which the animal's head is tracked better than 99% of the time during a complete 360-degree SPECT scan.

Future plans are to continue to develop pose measurement techniques that do not rely on the location of extrinsic markers, but intrinsic features of the animal such as the eyes and nose.

VI. REFERENCES

- [1] A.G. Weisenberger, B. Kross, S. Majewski, V. Popov, M.F. Smith, B. Welch R. Wojcik, S. Gleason, J. Goddard, M. Paulus, and S.R. Meikle, "Development and Testing of a Restraint Free Small Animal SPECT Imaging System with Infrared Based Motion Tracking," Proc. IEEE Medical Imaging Conference, November 2003.
- [2] J.S. Goddard, S.S. Gleason, M.J. Paulus, S. Majewski, V. Popov, M. Smith, A. Weisenberger, B. Welch, R. Wojcik, "Pose measurement and tracking system for motion-correction of unrestrained small animal PET/SPECT imaging," Proc. IEEE Medical Imaging Conference, November 2003.
- [3] A.G. Weisenberger, J.S. Baba, B. Kross, S. Gleason, J.S. Goddard, S. Majewski, S.R. Meikle, M. Paulus, M. Pomper, V. Popov, M.F. Smith, B. Welch, and R. Wojcik, "Dual Low Profile Detector Heads for a Restraint Free Small Animal SPECT Imaging System ", Proc. IEEE Nuclear Science Symposium and Medical Imaging Conference, Rome, Italy, October 2004.
- [4] Z. Zhang, "A flexible new technique for camera calibration," MSR-TR-98-71, Microsoft Research, Microsoft Corp., Redmond, WA, December 2, 1998.
- [5] D. Beque, J. Nuyts, G. Bormans, P. Suetens, P. Dupont, Characterization of pinhole SPECT acquisition geometry. IEEE Trans. Med Imag, Vol. 22, No 5, pp 599-612, May 2003.
- [6] D. Beque, J. Nuyts, G. Bormans, P. Suetens, P. Dupont, Optimization of SPECT Calibration, IEEE Medical Imaging Conference Record, Portland, 2003.
- [7] B. Horn, "Closed-form solution of absolute orientation using unit quaternions," Journal of the Optical Society of America, 4, pp. 629-642, April 1987.
- [8] R. Hartley and A. Zisserman, Multiple View Geometry in Computer Vision, Cambridge: Cambridge University Press, 2000.
- [9] O. Faugeras and Q-T. Luong, The Geometry of Multiple Images, Cambridge: The MIT Press, 2001.